Effect of microplasma irradiation on skin barrier function

Japanese Journal of Applied Physics **55**, 07LG01 (2016)
http://doi.org/10.7567/JJAP.55.07LG01

REGULAR PAPER

Effect of microplasma irradiation on skin barrier function

Kazuo Shimizu[1,2*], An N. Tran[1], and Marius Blajan[2]

[1]*Graduate School of Engineering, Shizuoka University, Hamamatsu 432-8561, Japan*
[2]*Organization for Innovation and Social Collaboration, Shizuoka University, Hamamatsu 432-8561, Japan*

*E-mail: shimizu@cjr.shizuoka.ac.jp

Received November 27, 2015; accepted February 13, 2016; published online June 14, 2016

In this paper, we introduce the feasibility of atmospheric-pressure argon microplasma irradiation (AAMI) to promote percutaneous absorption. A hairless Yucatan micropig skin was used for this ex vivo study. After AAMI, the disturbance in the stratum corneum (SC) lipids was observed using attenuated total reflectance-Fourier transform infrared spectroscopy. Also, an increase in transepidermal water loss and no physical damage on pig skins were confirmed by microscopic observation. These results of AAMI were compared with those of a plasma jet irradiation (PJI) and a tape stripping test (TST) leading to the conclusion that AAMI reduces the barrier function of the skin and could also enhance the transdermal absorption of drugs.

1. Introduction

The skin is the largest body organ, responsible for protecting the body from the external environment. Over time, there has been growing interest in skin penetration as a significant route for drug delivery, in which topical, regional, or systemic effects are desired.[1)] Skin penetration has advantages such as the stability of drug concentrations in the blood or avoiding first-pass metabolism and gastrointestinal drug degradation,[2,3)] but it is still limited to the delivery of small-molecule drugs and lipophilic drugs.[4,5)] For many years, various chemical, mechanical, and physical methods have been actively studied to enhance skin penetration, including ionphotoresis, sonophotoresis, and microneedles.[6)] However, besides the positive effects, cutaneous side effects of those methods were also reported.[7–9)] Therefore, safe and efficient transdermal permeation enhancement technology still remains a challenge in medicine and cosmetology.

Recently, atmospheric plasma applications have attracted attention due to their many potential advantages, such as the presence of highly reactive species[10–12)] [e.g., reactive oxygen species (ROSs) and reactive nitrogen species (RNSs)] and no requirement of costly vacuum enclosures. Particularly in the medical and biological fields, several recent studies have demonstrated that plasma is highly efficient for skin treatment,[13,14)] including skin disinfection[15–17)] and rejuvenation therapy.[18)]

Therefore, as an appropriate tool for skin treatment, we investigated the possibility of atmospheric-pressure argon microplasma irradiation (AAMI) for improving skin permeability. The other aim of this study is to investigate drug delivery through the skin without injection needles,[19)] without any damage to the skin.[20)] The impact of AAMI on the stratum corneum (SC), which plays an essential role in the barrier function of the skin, was examined in this study.[21)] In conclusion, this investigation indicates that AAMI is expected to be a promising alternative method that could promote drug delivery through the skin and could simultaneously minimize the pain from other skin penetration enhancement manipulations.

2. Materials and methods

2.1 Tissue samples

This ex vivo study was carried out on a hairless Yucatan micropig skin, which has similar permeability properties and histological characteristics to human skin.[22,23)] Frozen Yucatan micropig dorsal skin sheets (female pigs, 5 months old) were purchased from Charles River Japan Incorporated. The skin sheets were stored at −80 °C in a freezer until the series of measurements. Before starting each measurement, skin samples were equilibrated in a chamber at approximately 27 °C for 30 min and then utilized in full thickness.

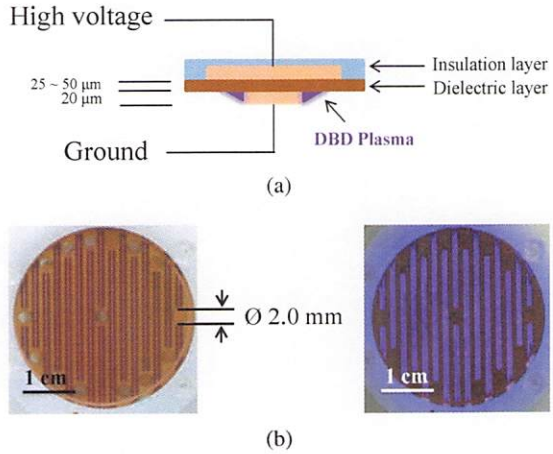

Fig. 1. (Color online) Images of microplasma electrodes. (a) Schematic image of cross-sectional view. (b) Top view of electrodes without plasma and with plasma discharge on the surface.

2.2 Microplasma generation

Figure 1 shows an image of a thin-film type electrode for AAMI.[24)] This electrode consists of a dielectric layer of roughly 25–50 μm thickness, sandwiched by two copper electrode layers. The high-voltage applied electrode was covered with an insulation layer and the grounded electrode faced the skin samples at a distance of 7 mm. The electrodes were perforated with 15 holes of 2.0 mm diameter allowing argon gas to pass through. Furthermore, the electrode was connected to the probe to maintain a stable supply of argon gas with a flow rate of 5 L/min for 1 and 5 min of microplasma irradiation (Fig. 2). Plasma was generated on the basis of dielectric barrier discharge (Fig. 3) at a low discharge voltage of 700 V (zero-to-peak, 27 kHz) using a neon-sign transformer (LECIP *α*NEON M-1H).

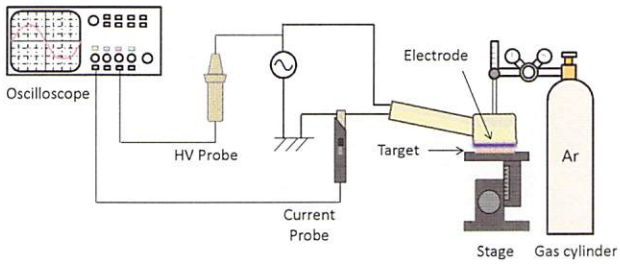

Fig. 2. (Color online) Experimental setup for atmospheric-pressure argon microplasma irradiation.

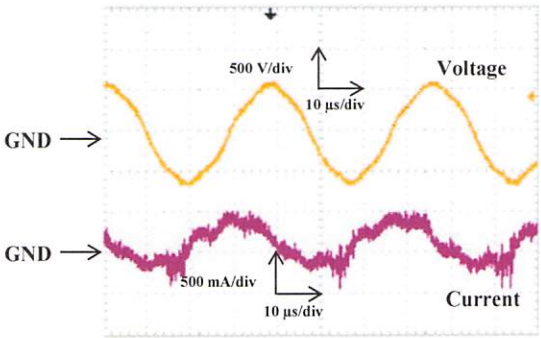

Fig. 3. (Color online) Applied AC high voltage and corresponding discharge current of microplasma.

2.3 Plasma jet irradiation and tape stripping test procedures

The effect of AAMI on skin was compared with that of a conventionally used plasma jet irradiation (PJI)[13,25–28] and a tape stripping test (TST). A schematic image of the plasma jet electrode is shown in Fig. 4(a). The electrode consists of a glass tube of 0.9 mm inner diameter (measured at the tip placement of the inner tungsten electrode), in which argon gas flows with a flow rate of 3 L/min. A plasma jet was also generated by the dielectric barrier discharge (DBD) that occurred between the tungsten electrode and the aluminum sheet wrapping the glass tube. Figure 4(b) shows an actual image of the light emission of this PJI. The exposure distance between the end of the glass tube and the pig skin surface was set at 7 mm. In this study, the procedures of PJI were carried out under the same experimental conditions as AAMI, however, the voltage was set at a discharge start voltage of 3.2 kV (zero-to-peak, 16.1 kHz) and the exposure time was 10 s.

TST is well known as a representative method for the evaluation of the barrier function of the SC and for the quantification of typically applied substances within the skin.[29–31] Layers of the SC were physically removed with every tape strip; hence, the barrier function of a skin sample will be decreased after this process. In this study, TST was carried out for 10 and 20 times on a pig skin surface with a pressure of 165 g/cm^2 using 3M Scotch Tape.[32]

2.4 Evaluation of skin barrier function

The changes in lipids and proteins in the pig SC were investigated using attenuated total reflectance-Fourier transform infrared (ATR-FTIR) spectroscopy (JASCO FT/IR 6300).[33,34] As shown in Fig. 5, the principle of the ATR method is based on the property of total internal reflection

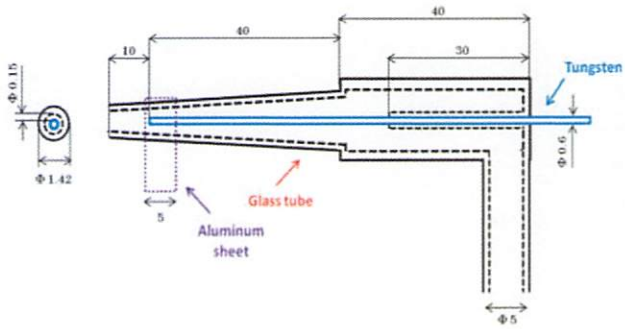

(a)

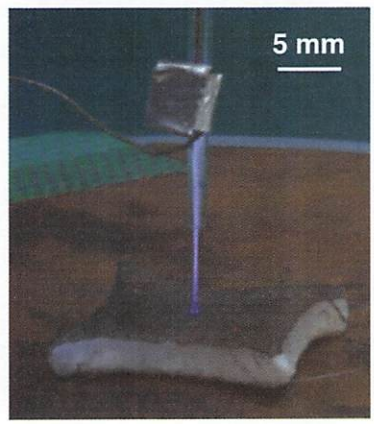

(b)

Fig. 4. (Color online) PJI procedure. (a) Schematic image of plasma jet electrodes. (b) Pig skin exposed to PJI.

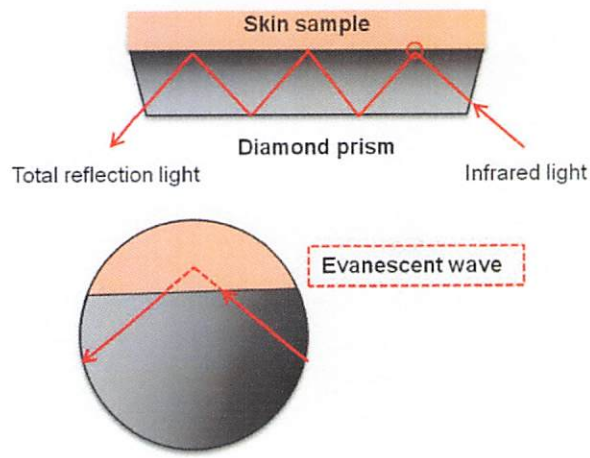

Fig. 5. (Color online) Basic principle of ATR method.

resulting in an evanescent wave, which is formed by the reflection of the infrared light off the internal surface, extending into the sample with a few micrometers in depth (0.5–5 μm). FTIR spectra were obtained by the measurement of this evanescent wave-induced attenuated energy.

In this study, ATR-FTIR analysis was conducted with a diamond prism. It has a higher refractive index (2.4) than that of the pig skin (1.55), which is required for the formation of total internal reflection at the interface.[35] For each analysis, 64 scans of infrared spectra were taken with a resolution of 4 cm^{-1}.

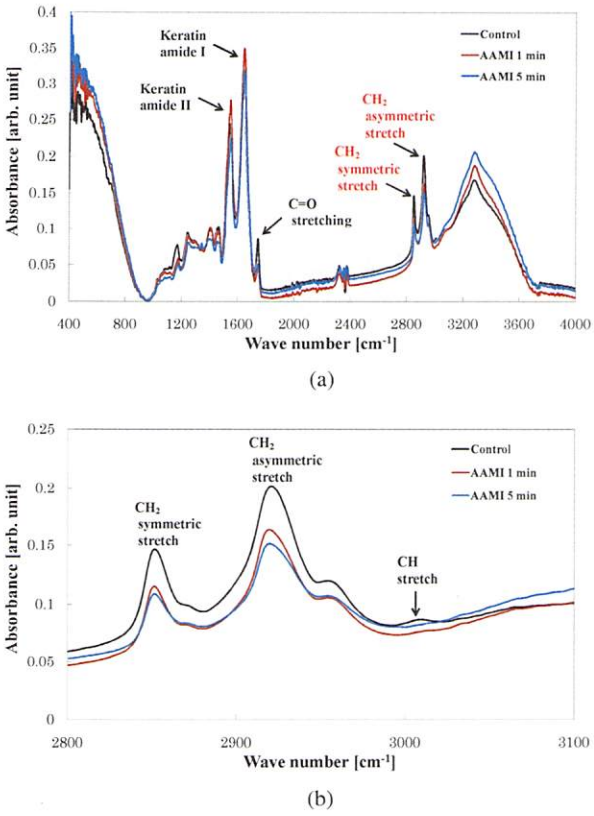

Fig. 6. (Color online) ATR-FTIR spectra. (a) Overall spectra of pig SC during AAMI. (b) Fragment of spectra focusing on methylene stretching vibration.

In addition, the barrier function alteration of the skin, which is correlated closely with the permeation behavior, was monitored by transepidermal water loss (TEWL) measurement[36,37] with an evaporimeter (Nikkiso Thermo H4500). A microscope (Leica DM IL LED) was also used to observe damage on pig skin samples.

3. Results and discussion

3.1 ATR-FTIR analysis

The alterations in the molecular structure of the SC after AAMI for 1 and 5 min elucidated by ATR-FTIR spectra are discussed below:

(i) The presence of amide III, II, and I absorbance peaks (near 1244, 1544, and 1644 cm^{-1}, respectively) arising from the keratin, which is the major protein of the corneocytes, was confirmed as shown in Fig. 6(a).[34] Amide I caused by the C=O stretching,[38] which correlates closely to the helical keratin secondary structure, had a higher absorbance intensity after AAMI. In addition, the shifted band in the amide III spectral range of 1200–1350 cm^{-1} could be produced by the different protein conformations.[39] Zhang et al. performed the oxidation on horn keratin using hydrogen peroxide and revealed that the oxidized keratin lost its ordered α-helical structure to form a disordered structure. Therefore, we also considered that AMMI could oxidize SC proteins resulting in the increase in both keratin amide I and II peaks.[40]

(ii) As shown in Fig. 6(b), a band assigned to =C–H stretching (roughly 3010 cm^{-1}) arising from unsaturated hydrocarbon chains,[34] was gradually disappearing after AAMI. The presence of the ester carbonyl stretching band at roughly 1740 cm^{-1} indicates that the unsaturated lipids including these unsaturated hydrocarbon chains were derived from sebum or contamination on the sample surface.[34] This band also significantly decreased, indicating that there was an ability of AMMI for skin cleansing.

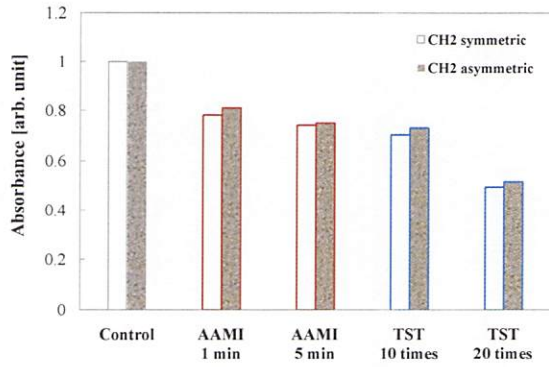

Fig. 7. (Color online) Comparison of decrease in CH_2 peaks between AAMI, TST, and PJI.

(iii) The absorbances in symmetric and asymmetric CH_2 stretching modes at approximately 2850 and 2920 cm^{-1} were chosen to evaluate the effect of AAMI on skin barrier function compared with those of TST and PJI. As shown in Fig. 7, the peak intensities were significantly decreased with the increase in the number of tape strips corresponding to the skin barrier defect. This decrease tendency of CH_2 stretching modes was also obtained in the case of AAMI. Moreover, the frequency of the symmetric methylene (CH_2) peak was shifted from 2850 to 2851 cm^{-1} after 5 min of AAMI, reflecting a change in the SC lipid conformation.[34]

For the plasma discharge in argon, the emission spectrum detected by Shimizu et al. shows the presence of excited Ar atoms, OH radicals, and O radicals.[41] In addition, other ROSs and RNSs could be generated during plasma discharge as a result of the presence of O_2 and N_2 in ambient air via the reactions below.[42,43]

$$OH + OH \rightarrow \mathbf{H_2O_2} \quad (1)$$

$$H_2O_2 + OH \rightarrow H_2O + \mathbf{O_2^-} + H^+ \quad (2)$$

$$O_2 + e^- \rightarrow 2\,O + e^- \quad (3)$$

$$O + O_2 + M \rightarrow \mathbf{O_3} + M \quad (4)$$

$$N_2 + e^- \rightarrow 2\,N + e^- \quad (5)$$

$$O_2 + e^- \rightarrow 2\,O + e^- \quad (6)$$

$$N + O\,(^3P) + M \rightarrow \mathbf{NO} + M \quad (7)$$

$$NO + OH \rightarrow \mathbf{NO_2^-} + H^+ \quad (8)$$

$$NO_2^- + O_3 \rightarrow \mathbf{NO_3^-} + O_2 \quad (9)$$

It has been accepted that ROSs have some effects on cell membranes and RNSs have an effect on biological cells. The above-mentioned ATR-FTIR analysis result indicated that AAMI could oxidize the SC protein and cause SC lipid disturbance. Thus, OH radicals and ROSs could be the main factors for improving skin permeability. However, the biological half-lives of typical reactive species such as H_2O_2 ($\sim 10^{-5}$ s), O_2^- ($\sim 10^{-6}$ s), OH radicals ($\sim 10^{-9}$ s), and NO (<1 s)[44] are not considerably long enough for their penetration through all the SC, which has a thickness of 10–40 μm.

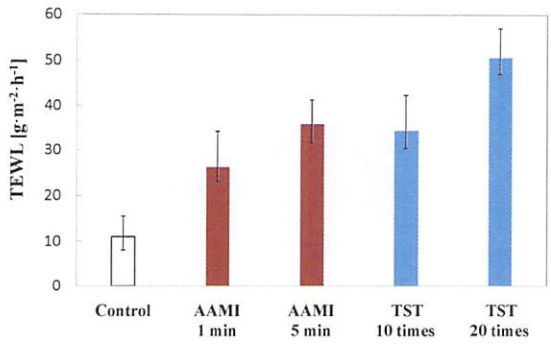

Fig. 8. (Color online) Variations in TEWL values before and after AAMI, TST, and PJI.

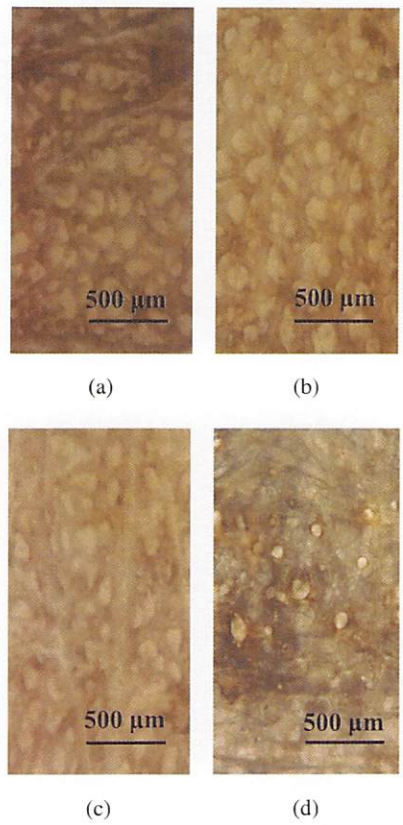

Fig. 9. (Color online) Microscopic photographs of YMP stratum corneum before and after the experiments: (a) control, (b) AAMI 5 min, (c) TST 20 times, and (d) PJI 10 s.

3.2 Assessment of skin barrier defects

A reduced epidermal barrier was also shown according to the increase in the TEWL value (Fig. 8). In addition, the TEWL value of AAMI 5 min ($35.92 \pm 3.48\,g{\cdot}m^{-2}{\cdot}h^{-1}$) was approximately the same as that of TST 10 times ($34.30 \pm 3.54\,g{\cdot}m^{-2}{\cdot}h^{-1}$), so the effect of these manipulations on the surfaces is considered to be at the same level.

The increase in the TEWL value compared with the control revealed that PJI also had an effect on the barrier function of the skin. Under the conditions of this study, PJI leads to a greater reduction in the barrier function of the skin even with a short exposure time (10 s). PJI had a direct etching effect on the sample surface caused by the flow of ionized gas with high-energy particles[45] leading to the formation of undesirable microholes, as shown in Fig. 9. In contrast, AAMI was a remote process, which could lead to less possibility of colliding charged particles on the sample surface. In addition, the differences in SC morphology shown in Fig. 9 could also be explained by the fact that while TST was a physical treatment, PJI was a combination of physical and chemical treatments. The increased TEWL value observed after several tests reflected and corresponded to the decrease in CH_2 peaks analyzed by ATR-FTIR methods.

Tero et al. revealed that DBD plasma irradiation induced pore formation (10 nm to 1 μm in size) in an artificial cell membrane system comprising supported lipid bilayers, which have a similar composition to intercellular lipid bilayers.[46] We also considered that the active species, charged species, or photons that existed in plasma could play a role to enhance drug penetration by the disturbance of the intercellular lipid bilayers. The disorder in this bilayer conformation, as shown in Fig. 10, could be considered to recover soon after plasma irradiation.

4. Conclusions

Owing to the presence of many highly reactive species (ROS, RNS, etc.), atmospheric-pressure argon microplasma irradiation is an efficient method to chemically modify a material substance. In this study, the effect of AAMI on SC lipid disorders was confirmed. This could lead to a feasible method of improving skin permeability and enhancing the transdermal absorption of drugs. Furthermore, AAMI does not cause undesirable damage to the skin and could be expected to minimize physical pain. These findings have indicated that there is feasibility of AAMI for medical applications and have provided a basis for future experimentation.

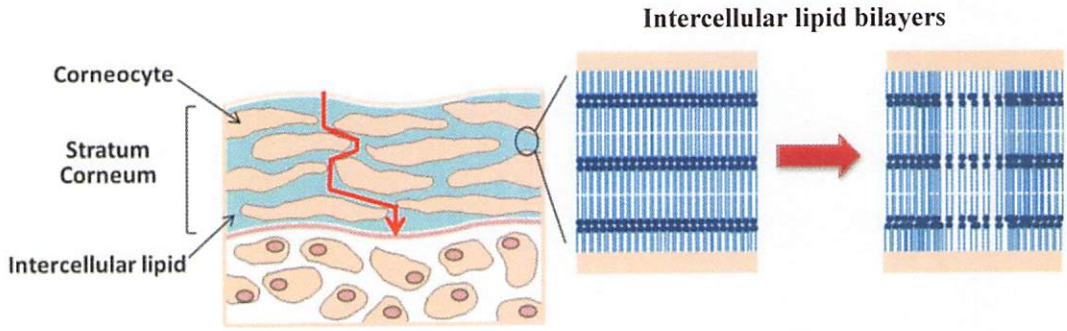

Fig. 10. (Color online) Conformational disorder of intercellular lipid bilayers by microplasma irradiation to the SC.

1) C. L. Dominguez Delgado, I. M. Rodriguez Cruz, and M. Lopez Cervantes, in *Current Technologies to Increase the Transdermal Delivery of Drugs*, ed. J. J. Escobar Chavez (Bentham Science Publishers, Shajah, 2010) Chap. 1.
2) I. L. O. Buxton and L. Z. Benet, in *Goodman and Gilman's The Pharmacological Basis of Therapeutics*, ed. L. L. Bruton, B. A. Chabner, and B. C. Knollmann (McGraw-Hill, New York, 2011) 12th ed., Chap. 2.
3) A. C. Anselmo and S. Mitragotri, J. Controlled Release **190**, 15 (2014).
4) M. R. Prausnitz and R. Langer, Nat. Biotechnol. **26**, 1261 (2008).
5) J. D. Bos and M. Meinardi, Exp. Dermatol. **9**, 165 (2000).
6) R. K. Subedi, S. Y. Oh, M.-K. Chun, and H.-K. Choi, Arch. Pharm. Res. **33**, 339 (2010).
7) G. L. Li, T. J. Van Steeg, H. Putter, J. Van Der Spek, S. Pavel, M. Danhof, and J. A. Bouwstra, Br. J. Dermatol. **153**, 404 (2005).
8) J. J. Escobar-Chavez, D. Bonilla-Martínez, M. A. Villegas-González, I. M. Rodríguez-Cruz, and C. L. Domínguez-Delgado, J. Pharm. Pharm. Sci. **12**, 88 (2009).
9) J. J. Escobar-Chávez, D. Bonilla-Martínez, M. Angélica, M. Villegas-González, E. Molina-Trinidad, N. Casas-Alancaster, and A. L. Revilla-Vázquez, J. Clin. Pharmacol. **51**, 964 (2011).
10) T. Adachi, H. Tanaka, S. Nonomura, H. Hara, S. Kondo, and M. Hori, Free Radical Biol. Med. **79**, 28 (2015).
11) I. Yagi, Y. Shirakawa, K. Hirakata, T. Akiyama, S. Yonemori, K. Mizuno, R. Ono, and T. Oda, J. Phys. D **48**, 424006 (2015).
12) D. B. Graves, J. Phys. D **45**, 263001 (2012).
13) G. Fridman, G. Friedman, A. Gutsol, A. B. Shekhter, V. N. Vasilets, and A. Fridman, Plasma Processes Polym. **5**, 503 (2008).
14) R. Hatakeyama and T. Kaneko, Plasma Fusion Res. **6**, 1106011 (2011).
15) J. Lademann, H. Richter, S. Schanzer, A. Patzelt, G. Thiede, A. Kramer, K. D. Weltmann, B. Hartmann, and B. Lange Asschenfeldt, Skin Pharmacol. Phys. **25**, 100 (2012).
16) J. Heinlin, G. Morfill, M. Landthaler, W. Stolz, G. Isbary, J. L. Zimmermann, T. Shimizu, and S. Karrer, J. Dtsch. Dermatol. Ges. **8**, 968 (2010).
17) O. Lademann, A. Kramer, H. Richter, A. Patzelt, M. C. Meinke, V. Czaika, K. D. Weltmann, B. Hartmann, and S. Koch, Skin Pharmacol. Phys. **24**, 284 (2011).
18) K. W. Foster, R. L. Moy, and E. F. Fincher, J. Cosmet. Dermatol. **7**, 169 (2008).
19) T. R. Kale and M. Momin, Innovations Pharm. **5**, 1 (2014).
20) J. Schramm and S. Mitragotri, Pharm. Res. **19**, 1673 (2002).
21) J. W. Wiechers, Pharm. Weekbl. **11**, 185 (1989).
22) K. Sato, K. Sugibayashi, and Y. Morimoto, J. Pharm. Sci. **80**, 104 (1991).
23) H. Takeuchi, S. Terasaka, T. Sakurai, A. Furuya, H. Urano, and K. Sugibayashi, Biol. Pharm. Bull. **34**, 555 (2011).
24) K. Shimizu, K. Hayashida, and M. Blajan, Biointerphases **10**, 029517 (2015).
25) A. Ando, H. Uno, T. Urisu, and S. Hamaguchi, Appl. Surf. Sci. **276**, 1 (2013).
26) D. L. Bayliss, J. L. Walsh, G. Shama, F. Iza, and M. G. Kong, New J. Phys. **11**, 115024 (2009).
27) Q. Y. Nie, Z. Cao, C. S. Ren, D. Z. Wang, and M. G. Kong, New J. Phys. **11**, 115015 (2009).
28) K. D. Weltmann, R. Brandenburg, T. Woetke, J. Ehlbeck, R. Foest, M. Stieber, and E. Kindel, J. Phys. D **41**, 194008 (2008).
29) H. L. Jenkins and J. A. Tresise, J. Soc. Cosmet. Chem. **20**, 451 (1969).
30) A. Teichmann, U. Jacobi, M. Ossadnik, H. Richter, S. Koch, W. Sterry, and J. Lademann, J. Invest. Dermatol. **20**, 264 (2005).
31) J. Lademann, U. Jacobi, C. Surber, H. J. Weigmann, and J. W. Fluhr, Eur. J. Pharm. Biopharm. **72**, 317 (2009).
32) H. Loffler, F. Dreher, and H. I. Maibach, Br. J. Dermatol. **151**, 746 (2004).
33) P. J. Caspers, G. W. Lucassen, and G. J. Puppels, Biophys. J. **85**, 572 (2003).
34) R. Mendelsohn, C. R. Flach, and D. J. Moore, Biochim. Biophys. Acta: Biomembranes **1758**, 923 (2006).
35) T. M. Greve, K. B. Andersen, and O. F. Nielsen, Spectrosc. Int. J. **22**, 437 (2008).
36) Z. Ya-Xian, T. Suetake, and H. Tagami, Arch. Dermatol. Res. **291**, 555 (1999).
37) K. Kikuchi, H. Kobayashi, T. Hirao, A. Ito, H. Takahashi, and H. Tagami, Dermatology **207**, 269 (2003).
38) W. K. Surewicz, H. H. Mantsch, and D. Chapman, Biochemistry **32**, 389 (1993).
39) F.-N. Fu, D. B. Deoliveira, W. R. Trumble, H. K. Sarkar, and B. R. Singh, Appl. Spectrosc. **48**, 1432 (1994).
40) Q. Zhang, G. Shan, P. Cao, J. He, Z. Lin, Y. Huang, and N. Ao, Mater. Sci. Eng. C **47**, 123 (2015).
41) K. Shimizu, M. Blajan, and S. Tatematsu, IEEE Trans. Ind. Appl. **48**, 1182 (2012).
42) K. Takahashi, Y. Sasaki, S. Mukaigawa, and K. Takaki, IEEE Trans. Plasma Sci. **38**, 2694 (2010).
43) C. A. J. van Gils, S. Hofmann, B. K. H. L. Boekema, R. Brandenburg, and P. J. Bruggeman, J. Phys. D **46**, 175203 (2013).
44) F. Marc, N. Marcus, W. Bo, and A. Oksana, Biochim. Biophys. Acta: Mol. Basis Dis. **1822**, 1363 (2012).
45) Th. von Woedtke, S. Reuter, K. Masur, and K. D. Weltnann, Phys. Rep. **530**, 291 (2013).
46) R. Tero, Y. Suda, R. Kato, H. Tanoue, and H. Takikawa, Appl. Phys. Express **7**, 077001 (2014).